Electrodialysis-based zero liquid discharge in industrial wastewater treatment

Jan Havelka, Hana Fárová, Tomáš Jiříček, Tomáš Kotala and Jan Kroupa

ABSTRACT

Over the past few decades, reverse osmosis (RO) has been the dominant technology employed in zero liquid discharge (ZLD) systems for industrial wastewater treatment (WWT). However, RO is limited to a maximum operating salinity of about 75 g kg^{-1}. Electrodialysis (ED) is a potentially attractive option as it can achieve much higher concentrations, thereby reducing the capacity and energy demand of the subsequent evaporation step. Feed-and-bleed experiments were undertaken on a laboratory-scale ED stack using a series of model solutions based on the most common inorganic salts with the aim of determining maximum achievable concentrations. The maximum salt concentration achievable via ED ranged between 104.2 and 267.6 g kg^{-1}, with levels predominantly limited by water transport. In addition, a straightforward review of how ED incorporation can affect ZLD process economics is presented. The operational cost of an ED-based ZLD system for processing RO retentate was almost 20% lower than comparable processes employing high-efficiency RO and disc tubular RO. As the ED-based ZLD system appears economically preferable, and as maximum achievable concentrations greatly exceeded RO operating limits, it would appear to be a promising approach for bridging the gap between RO and evaporation, and may even eliminate the evaporation step altogether.

Key words | brine, high concentration, maximum achievable concentration, wastewater, water transport coefficient

Jan Havelka (corresponding author)
Hana Fárová
Tomáš Jiříček
Tomáš Kotala
MemBrain s.r.o,
Pod Vinicí 87, 471 27 Stráž pod Ralskem,
Czech Republic
E-mail: *jan.havelka@membrain.cz*

Jan Kroupa
MEGA a.s.,
Pod Vinicí 87, 471 27 Stráž pod Ralskem,
Czech Republic

INTRODUCTION

Both the lack of freshwater and its quality have increasingly become global issues of our time (Subramani & Jacangelo 2014; Gosling & Arnell 2016; Mekonnen & Hoekstra 2016). Modern industry consumes vast amounts of freshwater and, in turn, produces huge quantities of wastewater with a high salt content. These waste brines, if not treated adequately, represent a severe threat to the environment. As ever-more stringent regulations are applied, a zero liquid discharge (ZLD) approach is being widely employed in industry in order to increase on-site water recycling and minimise liquid waste leaving the plant or facility (Schwarzenbach *et al.* 2010; Kim *et al.* 2013; Ahirrao 2014; Barrington & Ho 2014; Lin *et al.* 2015; Mansour *et al.* 2018).

Early ZLD initiatives were implemented at power plants near the Colorado River in the 1970s in order to treat increased salinity in the river water. In those days, thermal-based processes, such as brine concentrators, crystallisers, spray dryers and evaporation ponds, were the dominant ZLD systems used. However, such systems were prohibitively energy-intensive and required expensive metals for their construction to prevent scale and corrosion (Mickley 2008; Valdez & Schorr 2010; Tsai *et al.* 2017). Over the past few decades, reverse osmosis (RO) has been added to ZLD systems. While it is highly efficient and substantially less energy-demanding than thermal-based processes, its use is restricted to a maximum operating salinity of about 75 g kg^{-1}, mainly due to excessive osmotic pressure. Electrodialysis (ED), which is economically more feasible than thermal-based processes and achieves much higher salt concentrations than RO (being driven by an electric potential gradient), could prove a viable option for moving brine management forward (Shaffer *et al.* 2013; Tong & Elimelech 2016; Tsai *et al.* 2017; Shrivastava & Stevens 2018).

In this study, an array of typical salts present in industrial wastewaters was selected to determine the maximum achievable concentrations using ED, and the following scale-up

doi: 10.2166/wst.2019.161

parameters were examined: salt flux intensity, energy consumption and electric current efficiency. In addition, a simple economic study with real feed was performed.

METHODS

Equipment and operational conditions

A laboratory-scale ED stack consisting of standard heterogeneous cation (CMH-PES) and anion (AMH-PES) exchange membranes RALEX® (MEGA a.s., Czech Republic) with polyester (PES) support and polyethylene (PE) spacers (thickness 0.8 mm) was used to perform electrodialysis-high concentration (ED-HC) experiments (see Table 1 for basic membrane properties).

A laboratory P EDR-Z unit (MEGA a.s., Czech Republic) was used for the experiments. The ED stack was operated with a potential gradient of 1 V per cell pair and a current limiter corresponding to a current density of 250 A m^{-2}. The set-up consisted of three separate circuits, each with 2 L vessels for the diluate and concentrate solutions and a 0.25 L vessel for the electrode rinsing solution. Liquid flowrate in each circuit was set at 50 L h^{-1}. The ED stack typically consisted of 10 cell pairs with a total active membrane area of 0.064 m^2 and a linear velocity of 4.3 cm s^{-1}.

Based on industrial applications, the experiment was performed in feed-and-bleed mode, meaning that diluate conductivity was maintained at a level corresponding to a salt content of 10 g kg^{-1} by dosing fresh feed with a salt content of 50 g kg^{-1}, with concentrate conductivity increasing as a function of increasing salt content. The concentration of the appropriate salt in the electrode solution was set at 20 g kg^{-1}. The maximum salt concentration in the concentrate could never exceed that of a 'virtual' electroneutral solution transported through both membranes, thus giving an apparent concentration of salt inside the membranes ($c_{S,app}$). As the apparent concentration could not be measured, $c_{S,app}$ was determined in screening experiments from a mass balance according to Equation (2). The initial salt concentration (Table 2) was typically set at 0.9 $c_{S,app}$. Each experiment started with 0.5 kg of diluate, 0.5 kg of concentrate and 0.25 kg of electrode solution.

Sampling and analytical methods

All solutions for the ED-HC experiments were prepared using analytical grade chemicals (PENTA s.r.o., Czech Republic) dissolved in demineralised water with a conductivity of 8 μS cm^{-1}.

Flowrate, voltage, current, conductivity, pH, temperature and volume were measured on-site and recorded every 15 min. Flowrate was checked with an SK 52 variable area flow meter (Georg Fischer Ltd, Switzerland). Conductivity and temperature were measured with a TetraCon 325 electrode (WTW GmbH, Germany) and pH with a SenTix® 41 electrode (WTW GmbH, Germany), both of which were connected to a

Table 2 | List of salts tested in the ED-HC experiments and experimental set-up

Salt	Initial salt concentration in concentrate (g kg^{-1})	Electrode rinsing solution
Na_2SO_4	150	Na_2SO_4
K_2SO_4	100	K_2SO_4
NaCl	150	Na_2SO_4
NaCl:Na_2SO_4 (1:1)	150 (1:1)	Na_2SO_4
KCl	100	Na_2SO_4
$MgCl_2$	87	Na_2SO_4
NH_4Cl	145	Na_2SO_4
$NaNO_3$	200	$NaNO_3$
KNO_3	270	KNO_3
NH_4NO_3	224	$NaNO_3$
$Ca(NO_3)_2$	200	$NaNO_3$
$Mg(NO_3)_2$	150	$NaNO_3$
$NaHCO_3$	70	$NaNO_3$
$KHCO_3$	240	$KHCO_3$
NH_4HCO_3	190	$NaNO_3$

Table 1 | Basic properties of RALEX® membranes

Membrane	IEC[a] (meq g^{-1})	Permselectivity[b] (%)	Resistance[c] (Ω cm^2)	Thickness (mm)	pH range
CMH-PES	>2.2	>90	<8.0	<0.70	0–10[d]
AMH-PES	>1.8	>90	<7.5	<0.75	0–10[d]

[a]IEC: ion exchange capacity.
[b]Calculated from membrane potential measured across the membrane between 0.5 M and 0.1 M KCl solutions.
[c]Measured in 0.5 M NaCl at 25 °C.
[d]Except strong oxidising agents.

WTW Multi 340i multi-parameter instrument (WTW mbH, Germany). The volume of diluate and concentrate was obtained by reading the calibrated scale on the vessels.

Two samples were collected at the end of each experiment, one from the concentrate solution taken after draining the concentrate circuit and one from a mixture of the concentrate remainder and 0.5 kg of demineralised flushing water.

Gravimetric analysis, using a halogen moisture analyser HX204 (Mettler-Toledo GmbH, Switzerland), was used to determine the total dissolved solids content. Inductively coupled plasma (ICP) optical emission spectrometry (iCAP 7000 Series, Thermo Scientific, UK) was used for elemental analysis, while isotachophoresis (AGROFOR, JZD ODRA, Czech Republic) was used for anion analysis. Argentometry (0.1 M $AgNO_3$, indicator: K_2CrO_4) and neutralisation titrations (0.1 M HCl, indicator: methyl orange) were employed to determine Cl^- and HCO_3^-, respectively.

Calculations

The water transport coefficient (α_w) is the ratio of net water flux across the membrane vs. ionic flux, and can be defined by the equation (Nikonenko *et al.* 2012):

$$\alpha_W = \frac{1000 - c_{S,app}}{c_{S,app}} \quad (1)$$

where $c_{S,app}$ is the apparent concentration of salt inside the membranes (g kg^{-1}), evaluated continuously throughout the experiment from the mass balance based on the following equation:

$$c_{S,app}(t) = c_S(t) + m_C(t)\frac{dc_S}{dm_C}(t) \quad (2)$$

where c_S is the salt concentration in the concentrate (g kg^{-1}) derived as a function of electrical conductivity (κ_C), m_C is the mass of the concentrate (kg), both being functions of time (t). Density of the concentrate solution (ρ_C), derived as a function of salt concentration, was used to calculate mass from the concentrate solution volume (V_C).

The salt flux intensity (J_S) is an expression of the transport of salt in the membrane and is given as:

$$J_S = \frac{\Delta m_S}{A\ t_{tot}} \quad (3)$$

where Δm_S is the mass of salt transported from the diluate to the concentrate (g), A is the active membrane area (m^2) and t_{tot} is the time of electrodialysis (hours).

Energy consumption due to the electric current (E) in Wh per gram of transported salt was calculated from the equation:

$$E = \frac{\int_{t=0}^{t=t_{tot}} U(t)\ I(t)\ dt}{\Delta m_S} \quad (4)$$

where U is the actual voltage (V) and I is the actual direct current (A) during the experiment.

Electric current efficiency of the ED process (η) was evaluated as:

$$\eta = \frac{\Delta m_S\ z\ F}{M_S\ N\ I\ t_{tot}} \quad (5)$$

where z is the multiple of charge and stoichiometric coefficient of the ion, F is the Faraday constant (96,485 C mol^{-1}), M_S is the molar mass of salt and N is the number of cell pairs in the ED stack.

RESULTS AND DISCUSSION

Maximum achievable concentration

The experiments indicated that the maximum salt concentration achievable via ED is primarily influenced by its water transport coefficient (a result of ion hydration) and the salt's solubility in water (nucleation barrier). As examples, the maximum achievable concentration of $KHCO_3$ in water was limited by the apparent salt concentration inside the membranes $c_{S,app}$, while the solubility of $KHCO_3$ was almost 10 g kg^{-1} higher (Figure 1). On the

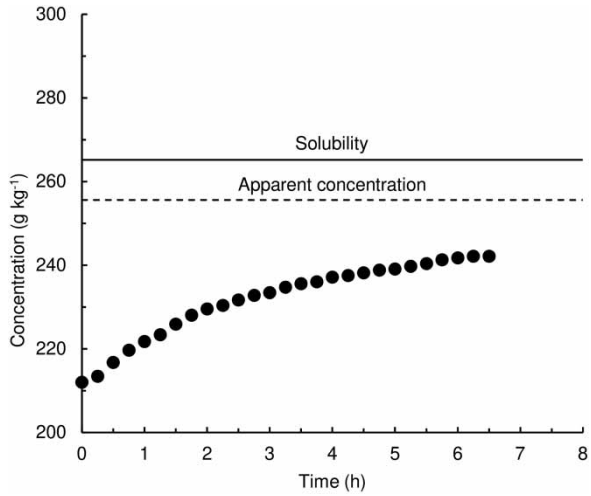

Figure 1 | Concentration of $KHCO_3$ in the concentrate solution over time during a single ED-HC experiment with a 10-pair stack.

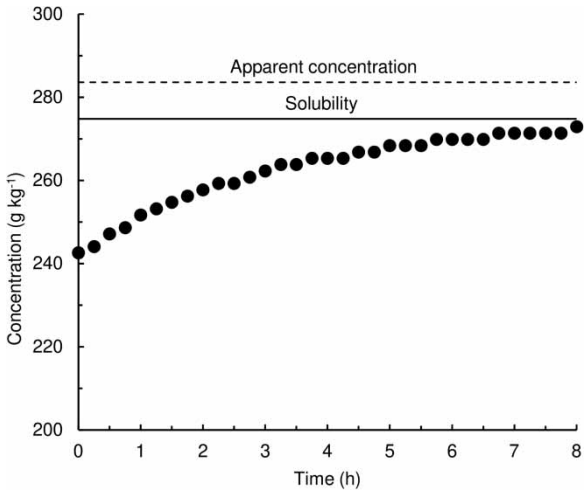

Figure 2 | Concentration of KNO_3 in the concentrate solution over time during a single ED-HC experiment with a 10-pair stack.

other hand, KNO_3 showed the opposite trend, with maximum achievable concentration within ED-HC limited by its solubility, which was approximately 8.8 g kg^{-1} lower than the apparent salt concentration (Figure 2). Most salts included in the experiment showed the same pattern as $KHCO_3$; only two other salts (K_2SO_4 and $NaHCO_3$) alongside KNO_3 were restricted from achieving higher concentrations by their solubility.

The maximum achievable concentrations for the array of salts tested ranged from 104.2 to 267.6 g kg^{-1} (Table 3). Based on these data, it can be concluded that ED can achieve higher concentrations for salts with lower water transport coefficients (e.g. KNO_3, $KHCO_3$ or NH_4NO_3), when not restricted by solubility. Even for salts with extremely high water transport coefficients (e.g. $MgCl_2$ or NH_4Cl), the maximum achievable concentration using ED greatly exceeded the RO operating limit (75 g kg^{-1}). However, pretreatment to prevent scaling from insoluble inorganic compounds (e.g. $CaCO_3$, $CaSO_4$) is still required under both processes to extend the lifetime of the equipment.

In the experiments using K_2SO_4, $NaHCO_3$ and NH_4HCO_3, the concentrate solution exceeded saturation levels by 20.4%, 10.6% and 3.2%, respectively. During operation, therefore, special attention should always be paid when solutions are above the saturation point.

Salt flux intensity

The active membrane area required for sufficient salt removal in an industrial application is dictated by the salt flux intensity, which depends on various parameters, such as the concentration gradient between diluate and concentrate solutions, linear velocity in ED stack, or applied voltage (Ghorbani & Ghassemi 2017). The study of the

Table 3 | Values for maximum achievable concentration ($c_{S,max}$), maximum molar fraction ($x_{S,max}$), water transport coefficient (α_w), salt intensity flux (J_S), energy consumption (E) and efficiency (η) for different salts used in the ED-HC experiments

Salt	$c_{S,max}$ (g kg^{-1})	$x_{S,max}$ (mol.%)	α_w (g_w g_s^{-1})	J_S (g m^{-2} h^{-1})	J_S (eq m^{-2} h^{-1})	E (Wh g_s^{-1})	η (%)
Na_2SO_4	193.1	2.95	4.0	550.0	7.74	0.40	86.0
K_2SO_4	129.0[a,b]	1.51	3.2	716.7	8.23	0.32	94.7
NaCl	175.0	6.14	4.0	576.0	9.86	0.40	75.0
NaCl:Na_2SO_4 (1:1)	160.5	4.08	4.6	490.5	7.81	0.45	80.0
KCl	186.3	5.24	3.8	505.1	6.76	0.36	73.0
$MgCl_2$	112.0	2.33	7.1	294.3	6.18	0.63	89.9
NH_4Cl	148.5	5.55	5.8	356.8	6.67	0.40	71.6
$NaNO_3$	227.6	5.88	3.3	605.8	7.13	0.40	77.8
KNO_3	267.6[a]	6.11	2.5	685.9	6.78	0.30	73.5
NH_4NO_3	229.6	6.29	3.1	473.6	5.92	0.34	63.7
$Ca(NO_3)_2$	208.7	2.81	3.3	510.4	6.22	0.39	81.9
$Mg(NO_3)_2$	173.8	2.49	4.3	461.1	6.22	0.43	83.8
$NaHCO_3$	104.2[a,b]	2.43	3.9	534.4	6.36	0.36	89.1
$KHCO_3$	242.7	5.45	2.9	780.8	7.80	0.30	84.0
NH_4HCO_3	205.1[b]	5.55	4.1	639.1	8.08	0.36	86.9

[a]Maximum achievable concentration is given by salt solubility.
[b]Concentration corresponding to supersaturated solution.

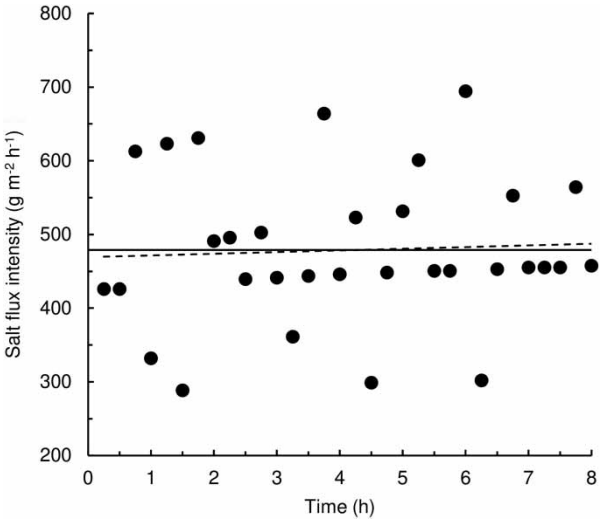

Figure 3 | Actual NH_4NO_3 flux intensity based on the difference in volume and conductivity of the concentrate solution vs. time. The dashed line represents linear regression and the solid line the average value calculated from the total mass balance.

effect of all these parameters on the salt flux intensity was beyond the scope of this paper, since under standard operating conditions very similar results were obtained for the majority of studied salts, ranging between 6 and 7 eq m^{-2} h^{-1} (Table 3). Such comparability should allow for simple ED scale-up of different salt mixtures. The actual value of the salt flux intensity did not vary over time, with any fluctuations in consecutive data points (see Figures 3 and 4) being caused by inaccuracies in concentrate volume measuring.

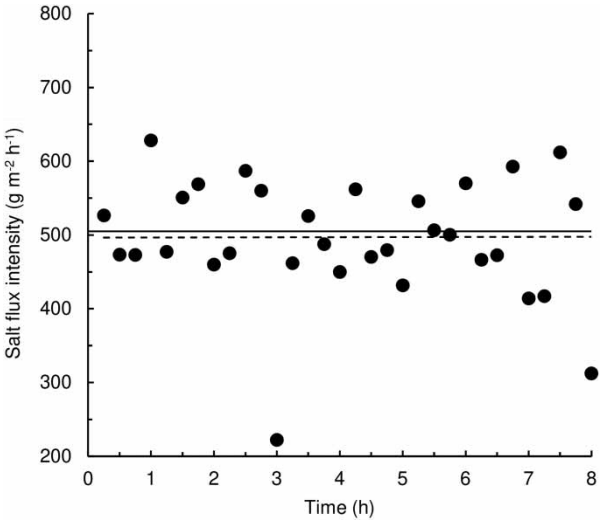

Figure 4 | Actual KCl flux intensity based on the difference in volume and conductivity of the concentrate solution vs. time. The dashed line represents linear regression and the solid line the average value calculated from the total mass balance.

Energy consumption and electric current efficiency

Values for energy consumption typically ranged between 0.36 and 0.40 Wh g_S^{-1} (Table 3). Both $Mg(NO_3)_2$ and the 1:1 mixture of NaCl and Na_2SO_4, however, required up to 20% more energy per gram of transported salt (though levels still did not exceed 0.45 Wh g_S^{-1}), while $MgCl_2$ was highly energy-demanding, at 0.63 Wh g_S^{-1}. This substantially higher energy demand compared with the other salts may be due to the formation of a viscous slurry (>97% of insoluble magnesium hydroxide $Mg(OH)_2$ as dry matter) on the cathode surface after dismantling the ED stack (Figure 5), which probably resulted in an increased electrical resistance for the module. Although ED of $Mg(NO_3)_2$ was also accompanied by formation of $Mg(OH)_2$ on the cathode surface, no significant increase in energy consumption was observed.

In more than half of the experiments the electric current efficiency was over 80%, the remaining salts (except NH_4NO_3) generally achieving more than 70% (Table 3). These values were highly dependent on the electric current passing through the stack, this being a function of the electrical resistance. Electrical resistance can be influenced by the ammonium pH equilibrium and by the formation of a precipitate, and these may have been responsible for the unusually low ED current efficiency of NH_4NO_3 and the high efficiency displayed by $MgCl_2$.

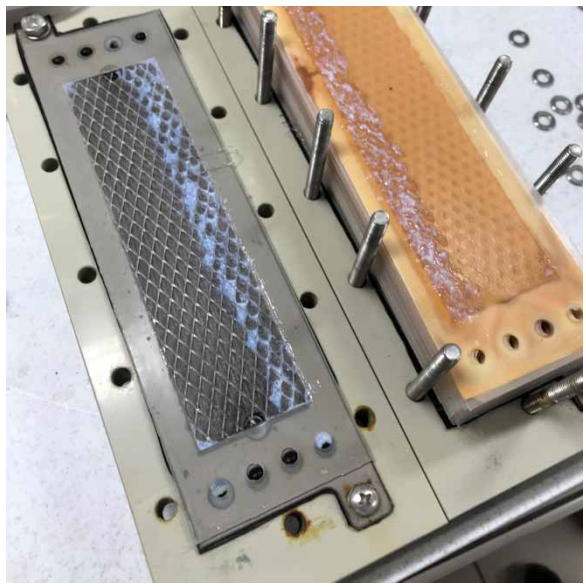

Figure 5 | Cathode rinsing cell after dismantling the stack. Note the right side of the electrode surface covered with a white viscous slurry (>97% $Mg(OH)_2$ dry matter).

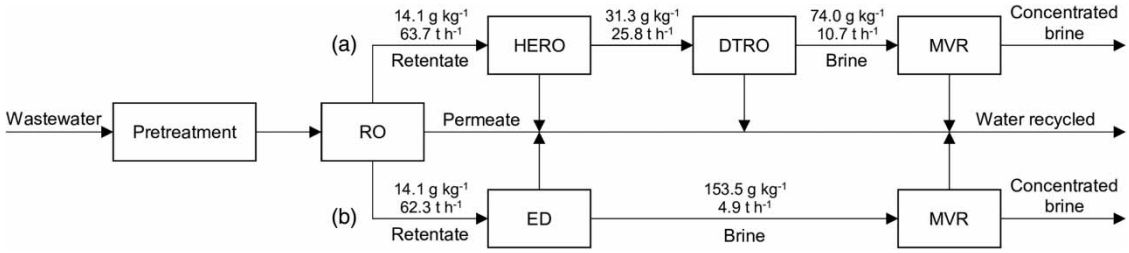

Figure 6 | Two different membrane-based ZLD system configurations for processing RO retentate: (a) HERO + DTRO + MVR; (b) ED + MVR.

Table 4 | OPEX estimates for two different ZLD systems processing RO retentate

	HERO + DTRO + MVR	ED + MVR
OPEX HERO stage (€ t^{-1} RO retentate)	0.207	–
OPEX DTRO stage (€ t^{-1} RO retentate)	0.219	–
OPEX ED stage (€ t^{-1} RO retentate)	–	0.560
OPEX MVR stage (€ t^{-1} RO retentate)	0.493	0.198
Total OPEX (€ t^{-1} RO retentate)	0.918	0.758

Economic study

An economic study of RO retentate processing capacity was performed for two different ZLD process trains (Figure 6). Although there are many innovative process routes covering both evaporative (multi-stage flash distillation, multi-effect distillation and membrane distillation) and non-evaporative (forward osmosis, pressure retarded osmosis and osmotically assisted RO) routes (Bartholomew *et al.* 2017; Osipi *et al.* 2018), this study does not compare them all as the majority of installations are built around the robust and trusted RO method. Hence, the first train was based on pressure driven membrane processes, including high-efficiency RO (HERO) and disc tubular RO (DTRO), followed by mechanical vapour recompression (MVR), while the second train was based on ED with MVR. The RO retentate was mainly composed of Na_2SO_4, $NaNO_3$ and NaCl, the amount of total dissolved solids (TDS) being 14.1 g kg^{-1}. Liquid flowrate of the RO retentate was 63.7 t h^{-1}.

Material balance and capital expenditure (CAPEX) for the first process train was based on commercial offers provided by equipment suppliers. The second process train was simulated by MEGA a.s. based on the laboratory scale data (Table 3). The laboratory membrane modules had identical length/width ratios and the same hydraulic regime as industrial stacks, with correction applied to compensate for the higher desalination rate along a longer liquid path in the industrial module. Moreover, only CAPEX was compared for the two installations, i.e. no buildings, utilities or transportation were taken into account. For this comparison, the price quotations are considered accurate, given that the equipment suppliers guarantee their capacities and product properties. Operating expenditure (OPEX) was calculated based on an energy price of 0.064 € kWh^{-1}.

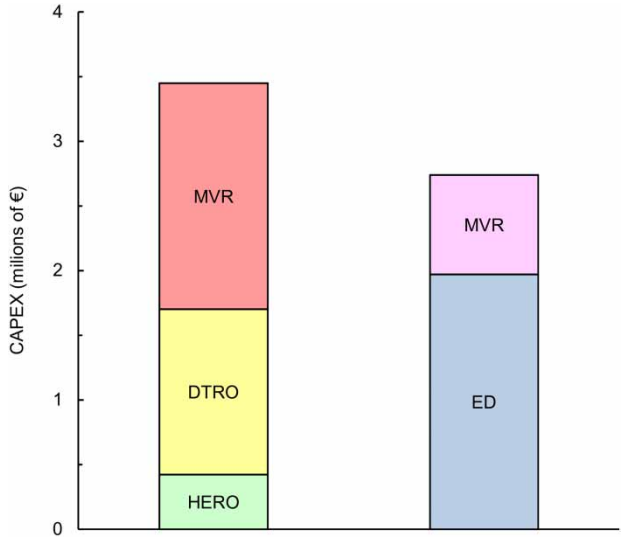

Figure 7 | Comparison of CAPEX for two different ZLD systems processing RO retentate.

Although ED energy consumption was higher than that of HERO + DTRO, overall OPEX for the second process train was much lower thanks to the reduced volume and higher salinity of the MVR feed (Table 4). The lower volume and higher salinity of the ED brine outlet also had a positive impact on MVR equipment size, and thus CAPEX (Figure 7).

CONCLUSION

Two parameters had a crucial impact on achieving high salt concentrations using ED: the water transport coefficient and salt solubility in water. Maximum achieved concentrations of model solutions greatly exceeded RO operating limits

and, in some cases, ED produced saturated or supersaturated solutions ready for final crystallisation. A simple economic study comparing two different ZLD systems (HERO + DTRO + MVR and ED + MVR) revealed that ED provided brine with a lower volume and higher salinity, thereby decreasing both the OPEX and CAPEX of the subsequent MVR. These findings support the technical and economic superiority of ED for pressure driven ZLD systems.

ACKNOWLEDGEMENTS

This study was undertaken under the framework of Project LO1418 'Progressive Development of Membrane Innovation Centre', supported by the Program NPU I of the Ministry of Education, Youth and Sports of the Czech Republic, using the infrastructure of the Membrane Innovation Centre.

REFERENCES

Ahirrao, S. 2014 Zero Liquid Discharge Solutions. In: *Industrial Wastewater Treatment, Recycling and Reuse*, 1st edn (V. V. Ranade & V. M. Bhandari, eds). Butterworth-Heinemann, Oxford, UK, pp. 489–520. DOI: 10.1016/B978-0-08-099968-5.00013-1.

Barrington, D. J. & Ho, G. 2014 Towards zero liquid discharge: the use of water auditing to identify water conservation measures. *Journal of Cleaner Production* **66**, 571–576. DOI: 10.1016/j.jclepro.2013.11.065.

Bartholomew, T. V., Mey, L., Arena, J. T., Siefert, N. S. & Mauter, M. S. 2017 Osmotically assisted reverse osmosis for high salinity brine treatment. *Desalination* **421**, 3–11. DOI: 10.1016/j.desal.2017.04.012.

Ghorbani, A. & Ghassemi, A. 2017 Brackish water desalination using electrodialysis: predictive mass transfer and concentration distribution model along the electrodialyzer. *Water Science and Technology* **77** (3), 597–607. DOI: 10.2166/wst.2017.547.

Gosling, S. N. & Arnell, N. W. 2016 A global assessment of the impact of climate change on water scarcity. *Climatic Change* **134**, 371–385. DOI: 10.1007/s10584-013-0853-x.

Kim, E.-S., Dong, S., Liu, Y. & Gamal El-Din, M. 2013 Desalination of oil sands process-affected water and basal depressurization water in Fort McMurray, Alberta, Canada: application of electrodialysis. *Water Science and Technology* **68** (12), 2668–2675. DOI: 10.2166/wst.2013.533.

Lin, J., Ye, W., Zeng, H., Yang, H., Shen, J., Darvishmanesh, S., Luis, P., Sotto, A. & Van der Bruggen, B. 2015 Fractionation of direct dyes and salts in aqueous solution using loose nanofiltration membranes. *Journal of Membrane Science* **477**, 183–193. DOI: 10.1016/j.memsci.2014.12.008.

Mansour, F., Alnouri, S. Y., Al-Hindi, M., Azizi, F. & Linke, P. 2018 Screening and cost assessment strategies for end-of-Pipe Zero Liquid Discharge systems. *Journal of Cleaner Production* **179**, 460–477. DOI: 10.1016/j.jclepro.2018.01.064.

Mekonnen, M. M. & Hoekstra, A. Y. 2016 Four billion people facing severe water scarcity. *Science Advances* **2** (2), e1500323–e1500323. DOI: 10.1126/sciadv.1500323.

Mickley, M. 2008 *Survey of High-Recovery and Zero Liquid Discharge Technologies for Water Utilities*. Water Reuse Foundation, Alexandria, VA, USA.

Nikonenko, V. V., Yaroslavtsev, A. B. & Pourcelly, G. 2012 Ion transfer in and through charged membranes: structure, properties, and theory. In: *Ionic Interactions in Natural and Synthetic Macromolecules*, 1st edn (A. Ciferri & A. Perico, eds). John Wiley & Sons, Inc., Hoboken, New Jersey, USA, pp. 267–335. DOI: 10.1002/9781118165850.ch9.

Osipi, S. R., Secchi, A. R. & Borges, C. P. 2018 Cost assessment and retro-techno-economic analysis of desalination technologies in onshore produced water treatment. *Desalination* **430**, 107–119. DOI: 10.1016/j.desal.2017.12.015.

Schwarzenbach, R. P., Egli, T., Hofstetter, T. B., von Gunten, U. & Wehrli, B. 2010 Global water pollution and human health. *Annual Review of Environment and Resources* **35**, 109–136. DOI: 10.1146/annurev-environ-100809-125342.

Shaffer, D. L., Arias Chavez, L. H., Ben-Sasson, M., Romero-Vargas Castrillón, S., Yip, N. Y. & Elimelech, M. 2013 Desalination and reuse of high-salinity shale gas produced water: drivers, technologies, and future directions. *Environmental Science & Technology* **47** (17), 9569–9583. DOI: 10.1021/es401966e.

Shrivastava, A. & Stevens, D. 2018 Energy efficiency of reverse osmosis. In: *Sustainable Desalination Handbook*, 1st edn (V. G. Gude, ed.). Butterworth-Heinemann, Oxford, UK, pp. 25–54. DOI: 10.1016/B978-0-12-809240-8.00002-2.

Subramani, A. & Jacangelo, J. G. 2014 Treatment technologies for reverse osmosis concentrate volume minimization: a review. *Separation and Purification Technology* **122**, 472–489. DOI: 10.1016/j.seppur.2013.12.004.

Tong, T. & Elimelech, M. 2016 The global rise of zero liquid discharge for wastewater management: drivers, technologies, and future directions. *Environmental Science & Technology* **50** (13), 6846–6855. DOI: 10.1021/acs.est.6b01000.

Tsai, J.-H., Macedonio, F., Drioli, E., Giorno, L., Chou, C.-Y., Hu, F.-C., Li, C.-L., Chuang, C.-J. & Tung, K.-L. 2017 Membrane-based zero liquid discharge: myth or reality? *Journal of the Taiwan Institute of Chemical Engineers* **80**, 192–202. DOI: 10.1016/j.jtice.2017.06.050.

Valdez, B. & Schorr, M. 2010 Corrosion control in the desalination industry. *Advanced Materials Research* **95**, 29–32. DOI: 10.5772/14054.

First received 2 November 2018; accepted in revised form 25 April 2019. Available online 6 May 2019